Multistability and condensation of exciton-polaritons below threshold

Jiun-Yi Lien,[1,2,*] Yueh-Nan Chen,[1,†] Natsuko Ishida,[3] Hong-Bin Chen,[1] Chi-Chuan Hwang,[2] and Franco Nori[3,4]
[1]*Department of Physics and Center for Theoretical Sciences, National Cheng Kung University, Tainan 701, Taiwan*
[2]*Department of Engineering Science, National Cheng Kung University, Tainan 701, Taiwan*
[3]*CEMS, RIKEN, Wako-shi, Saitama 351-0198, Japan*
[4]*Physics Department, University of Michigan, Ann Arbor, Michigan 48104-4313, USA*
(Received 16 July 2014; revised manuscript received 8 January 2015; published 20 January 2015)

Exciton-polaritons can condense to a macroscopic quantum state through a nonequilibrium process of pumping and decay. In recent experiments, polariton condensates are used to observe, for a short time, nonlinear Josephson phenomena by coupling two condensates. However, it is still not clear how these phenomena are affected by the pumping and decay at long times and how the coupling alters the polariton condensation. Here, we consider a polariton Josephson junction pumped on one side and study its dynamics within the mean-field theory. The Josephson current is found to give rise to multistability of the stationary states, which are sensitive to the initial conditions and incoherent noises. These states can be attributed to either the self-trapping effect or the parity-time (PT) symmetry of the system. These results can be used to explain the emission spectra and the π-phase locking observed in recent experiments. We further predict that the multistability can reduce to the self-trapped state if the PT symmetry is broken. Moreover, the polaritons can condense even below the threshold, exhibiting hysteresis.

DOI: 10.1103/PhysRevB.91.024511 PACS number(s): 03.75.Kk, 71.36.+c

I. INTRODUCTION

Exciton-polaritons, i.e., quasiparticles composed of cavity photons and quantum-well excitons in semiconducting microcavities, have recently been demonstrated to form Bose-Einstein condensates (BECs) due to their light effective mass originating from the photonic part [1–5]. The exciton-polariton BEC can be used to investigate macroscopic quantum effects in semiconducting systems, such as superfluidity [6,7] and quantized vortices [8,9]. In addition, the well-known Josephson effects can be exhibited in a bosonic Josephson junction (BJJ), i.e., two coherently coupled condensates confined in a double-well potential. Besides the phase-difference-induced current (dc effect) and the detuning-induced oscillations (ac effect) observed in superconducting and helium superfluid systems, the interaction between the condensate bosons leads to nonlinear effects when the boson number increases, such as anharmonic oscillations and initial-imbalance-induced trapping toward one site (called macroscopic quantum self-trapping) [10]. These phenomena were first observed in ^{87}Rb condensates [11] and have also been demonstrated recently in exciton-polariton BJJs with disordered double wells [12] and semiconductor micropillars [13].

Since the lifetime of exciton-polaritons is tens to hundreds of picoseconds, an optical pumping is necessary to compensate both the radiative and the nonradiative decay of the polaritons. Therefore, the condensates are formed in such a nonequilibrium process. At low temperatures, one can use a nonresonant pumping to excite higher-energy excitons, which rapidly relax to form an incoherent polariton reservoir at the bottleneck of the lower-energy polariton band through the exciton-phonon interactions. The polaritons are then stimulatedly scattered (or cooled) into the ground state to achieve condensation with spontaneous coherence, provided that the incoherent polariton density reaches the threshold density [1,14]. The polariton reservoir drastically changes the Bogoliubov dispersion of the elementary excitations for condensates with conserved particle numbers, leading to a diffusive behavior in the long-wavelength regime and the dynamical instability of the reservoir lifetime's being comparable to that of the condensate [15,16].

While the dynamics of the polariton BJJ for different regimes can be accessed by a pulsed resonant excitation that gives the appropriate initial conditions [13], the short-time behavior of the polariton BJJ is also affected by the reservoir, e.g., the spontaneous coherent oscillations driven by a nonresonant pumping covering the double well [12]. In addition to these short-time oscillations, the nonequilibrium process with a continuous-wave pumping laser would also alter the behavior at long times. It has been reported [17] that under equivalent pumping on both sides, the synchronization of the condensates with a single eigenenergy can be destroyed by the potential difference across the junction, where a long-time ac Josephson oscillation exists in the desynchronized phase [18]. A similar synchronization-desyncronization phase transition was also observed [19] in microcavities with in-plane disorder.

In this work, we consider a different situation: a polariton BJJ with a single nonresonant pumping focused on one side [Fig. 1(a)]. This has been realized in recent experiments using a pumping laser with a small enough spot size [13,20]. In contrast with the regime under equivalent pumping [17,18], no ac Josephson oscillations are found even in the presence of a potential difference. We present the multiple stability induced by the Josephson current, as well as its effect on the threshold pumping. Furthermore, we also find the possibility of condensation even below the threshold.

II. GENERALIZED GROSS-PITAEVSKII EQUATIONS

Our analysis is based on the generalized Gross-Pitaevskii equation of the BJJ wave functions $\vec{\Psi} \equiv (\Psi_1, \Psi_2)^T \equiv (\sqrt{N_{c1}}e^{i\varphi_1}, \sqrt{N_{c2}}e^{i\varphi_2})^T$,

$$i\frac{d}{dt}\vec{\Psi} = H\vec{\Psi}, \tag{1}$$

*jiunyi.lien@gmail.com
†yuehnan@mail.ncku.edu.tw

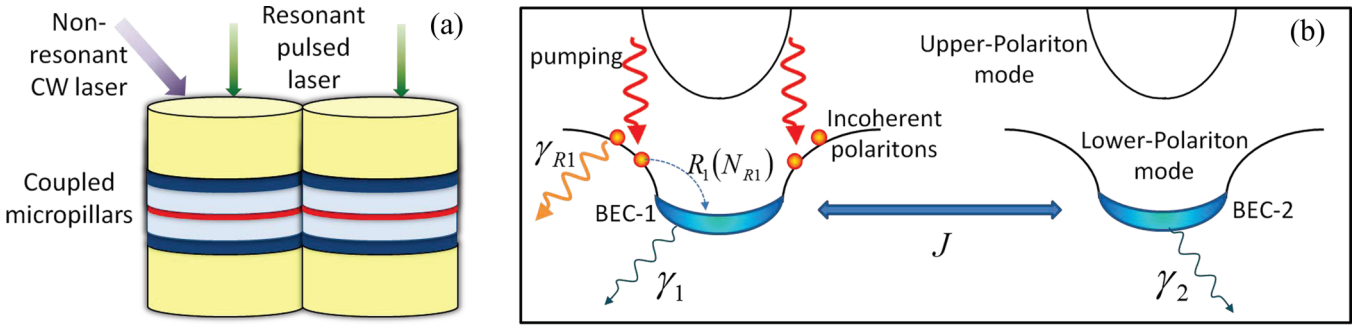

FIG. 1. (Color online) (a) A polariton Josephson junction made of semiconducting micropillars pumped on one side. (b) Model of exciton-polariton condensation of the junction. A nonresonant continuous-wave laser is used to excite high-energy excitons as a pumping to the polariton reservoir, and a resonant pulsed laser can be used to control the initial condition.

coupled to a rate equation describing the reservoir [16,17]. The nonlinear and non-Hermitian Hamiltonian is written as

$$H \equiv \begin{pmatrix} E_1 & -J \\ -J & E_2 \end{pmatrix}, \qquad E_j \equiv \epsilon_j + V_j(N_{Rj}) + U_j|\Psi_j|^2, \tag{2}$$

where ϵ_j is the single-particle ground-state energy, U_j is the condensate charging energy, and J is the tunneling between the two sites. Here the local dispersion is ignored and we only consider the ground-state wave function of each site, as shown in Fig. 1(b).

The complex effective potential V_j is given by

$$V_j\left(N_{Rj}\right) \equiv \left(\frac{\tilde{g}}{A_j}N_{Rj} + \mathcal{G}_j P_j\right) + \frac{i}{2}[R_j(N_{Rj}) - \gamma_j] \equiv V_j^R(N_{Rj}) + i V_j^I(N_{Rj}), \tag{3}$$

and it depends on the number of reservoir polaritons $N_{Rj}(t)$ and the pumping strength P_j, where $\tilde{g}$ is the interaction between the condensate and the reservoir polaritons, A_j is approximately the distribution area of the reservoir, $\mathcal{G}_j$ corresponds to the interaction between the condensate and the high-energy excitons [21], and γ_j is the decay of the condensates. The term $R_j(N_{Rj})$ is the stimulated scattering from the reservoir to the condensate, and for simplicity, we only consider it as a linear function, i.e., $R_j(N_{Rj}) \equiv R_j' N_{Rj}$.

The rate equation of the reservoir on the pumped site is given by

$$\frac{d}{dt}N_{R1} = P_1 - \gamma_{R1}N_{R1} - R_1(N_{R1})|\Psi_1|^2, \tag{4}$$

where the reservoir decay γ_{R1} and scattering loss are balanced by the laser pumping P_1. We can ignore N_{R2} due to the weak diffusion of the reservoir polaritons [16]. The interaction terms in V_j^R can be treated as the effective potential energies together with ϵ_j. We ignore ϵ_j and V_j^R in Sec. III, and the effects of these potential differences (detuning) are discussed in Sec. V A.

III. STATIONARY STATES

A. Noncondensed solutions

A trivial solution is that no polaritons are condensed and the reservoir-polariton number is proportional to the pumping from (4). By linearizing Eq. (1), the fluctuation spectrum can be derived as

$$\omega_\pm^{(0)} = \frac{1}{2}\left(E_1^{(0)} + E_2^{(0)}\right) \pm \frac{1}{2}\sqrt{\left(E_1^{(0)} - E_2^{(0)}\right)^2 + 4J^2}, \tag{5}$$

where $E_j^{(0)}$ is given by Eq. (2) with $\vec{\Psi} = 0$. As shown in Fig. 2, the threshold pumping $P_{\rm th} = \gamma_{R1}N_{R\rm th}$ can be determined by the first point of $\mathrm{Im}[\omega_\pm^{(0)}] = 0$, where the noncondensed solution becomes unstable. For $J = 0$, the threshold reduces to the single-BEC case with $R_1(N_{R\rm th}) = \gamma_1$. It increases with J until $N_{R\rm th}$ reaches a saturation point with $R_1(N_{R\rm th}) = \gamma_1 + \gamma_2$.

B. Real spectrum of the condensates

In general, the spectrum of the non-Hermitian Hamiltonian H is a complex function of the polariton numbers of the condensates and the reservoir. To solve the nonzero stationary states, $\vec{\Psi}(t) \equiv \vec{\Psi}(0)e^{-i\Omega t}$, and N_{R1}, we have to search for the real spectrum, i.e.,

$$\Omega_\pm = \frac{1}{2}(E_1 + E_2) \pm \frac{1}{2}\sqrt{(E_1 - E_2)^2 + 4J^2} \in \mathbb{R}. \tag{6}$$

The stationary states pumped from one side must possess a finite dc Josephson current $2J\sqrt{N_{c1}N_{c2}}\sin(\Delta\varphi)$ to balance the loss from the other side, and the relative phase $\Delta\varphi \equiv \varphi_2 - \varphi_1$ across the BJJ (with respect to Ω_- and Ω_+) deviates from 0 and π, corresponding to the usual bonding and antibonding states with zero current.

Two analytic solutions can be derived from $R_1(N_{R1}) = \gamma_1 + \gamma_2$; one corresponds to Ω_+ and the other to Ω_- [see thick solid (yellow) and long-dashed (green) curves in Fig. 3]. In this case, the Hamiltonian possesses parity-time (PT) symmetry, i.e., $E_1 = E_2^*$, where the injection of the condensate polaritons at site 1, $R_1(N_{R1}) - \gamma_1$, is equal to the decay at site 2 [22,23]. These stationary states only exist with a real spectrum under the condition

$$J^2 \geqslant \frac{1}{16}\left[R_1(N_{R1}) - \gamma_1 + \gamma_2\right]^2 = \frac{\gamma_2^2}{4}. \tag{7}$$

Violating this condition by increasing the decay or decreasing the tunneling makes the spectrum complex and leads to *spontaneous PT-symmetry breaking* [23–27]. The equal sign in Eq. (7) gives the exceptional point, where these two states coalesce.

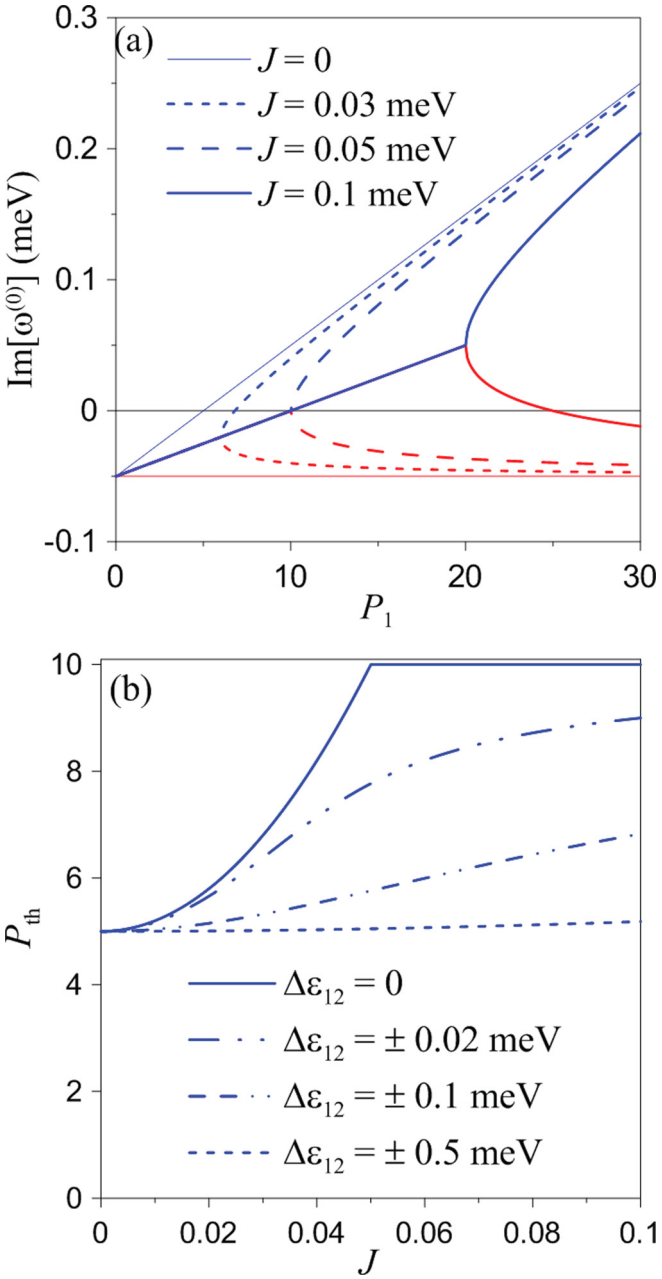

FIG. 2. (Color online) (a) Imaginary part of the excitation spectrum $\omega^{(0)}$ without condensation. (b) Threshold pumping $P_{\rm th}$ as a function of the Josephson coupling strength J with and without the detuning $\Delta\varepsilon_{12}$, where $P_{\rm th}$ is defined as the first point of $\mathrm{Im}[\omega_{\pm}^{(0)}] = 0$ in (a). The decay rates are $\gamma_1 = \gamma_2 = 0.1$ meV, which are close to those in the micropillar experiment, $\gamma_{R1} = 0.5$ meV and $R_1' = 0.01$ meV.

For both PT-symmetric states, the condensate polaritons are equally populated across the junction,

$$|\Psi_1|^2 = |\Psi_2|^2 = \frac{P_1 - \gamma_{R1} N_{R1}}{R_1(N_{R1})}. \tag{8}$$

By coincidence, these states are created above the threshold because the reservoir polaritons have to be pumped to the condition $N_{R1} = N_{R\rm th}$. The reservoir-polariton number is kept constant above the threshold and the total condensate-polariton number ($N_{cT} \equiv N_{c1} + N_{c2}$) increases linearly with the pumping [Figs. 3(b) and 3(c)].

In general, there exist two other solutions, both corresponding to Ω_+, with an imbalanced population of condensate polaritons $\zeta \equiv (N_{c1} - N_{c2})/N_{cT} \neq 0$ [Fig. 3(d)]. They are obtained by numerically finding the roots of $\mathrm{Im}(\Omega) = 0$. One solution is localized at site 1 [thin solid (blue) curves in Fig. 3], and this localization is due to the same mechanism of macroscopic quantum self-trapping for short-time oscillations [10], where the interaction between the condensate polaritons shifts the energy difference across the BJJ and reduces the Josephson current. Therefore, increasing the pumping or decreasing the junction tunneling enhances the self-trapping effect. The other solution is more populated at site 2 with weaker condensation [dot-dashed (red) curves in Fig. 3] and the self-trapping effect is limited. Increasing the pumping will drive more polaritons tunneling to the unpumped site and further reduce the condensation. Thus, the solution reduces to the zero-condensate state above a critical pumping. Interestingly, the imbalanced states appear even below the threshold. We show later that the polariton BJJ exhibits bistability below the threshold.

C. Multiple stability

In order to determine which states can be observed experimentally, the stability is analyzed by calculating the complex spectrum of deviation from stationary states. However, we do not employ the usual derivation of the elementary excitations by directly linearizing Eq. (1), which includes both phase terms, φ_1 and φ_2. This is because only the phase difference is physically meaningful without considering the local dispersion. Instead, we derive the equations of motion of the phase difference $\Delta\varphi$ and the population imbalance ζ, similar to the conserved BEC systems [10], and take into account the additional degrees of freedom, i.e., the total condensate-polariton number N_{cT} and the reservoir-polariton number N_{R1}. The equations of motion are given by

$$\begin{aligned}
\dot{\zeta} &= V_{12}^I(1-\zeta^2) - 2J\sqrt{1-\zeta^2}\sin(\Delta\varphi),\\
\Delta\dot{\varphi} &= \epsilon_{12} + V_{12}^R + \left(\frac{U_{12}}{2} + \bar{U}\zeta\right) N_{cT}\\
&\quad + 2J\frac{\zeta}{\sqrt{1-\zeta^2}}\cos(\Delta\varphi),\\
\dot{N}_{cT} &= \left[2\bar{V}^I + V_{12}^I\zeta\right] N_{cT},\\
\dot{N}_{R1} &= P_1 - \gamma_{R1}N_{R1} - R_1(N_{R1})N_{cT}\frac{1+\zeta}{2},
\end{aligned} \tag{9}$$

where

$$\begin{aligned}
\bar{U} &\equiv \frac{U_1 + U_2}{2},\\
U_{12} &\equiv U_1 - U_2,
\end{aligned} \tag{10}$$

and similar definitions are applied to $V_j^{R/I}$ and ϵ_j. The term $\epsilon_{12} + V_{12}^R$ corresponds to the effective detuning including the reservoir polaritons and high-energy excitons. By linearizing Eq. (9), we can calculate the fluctuation spectrum and

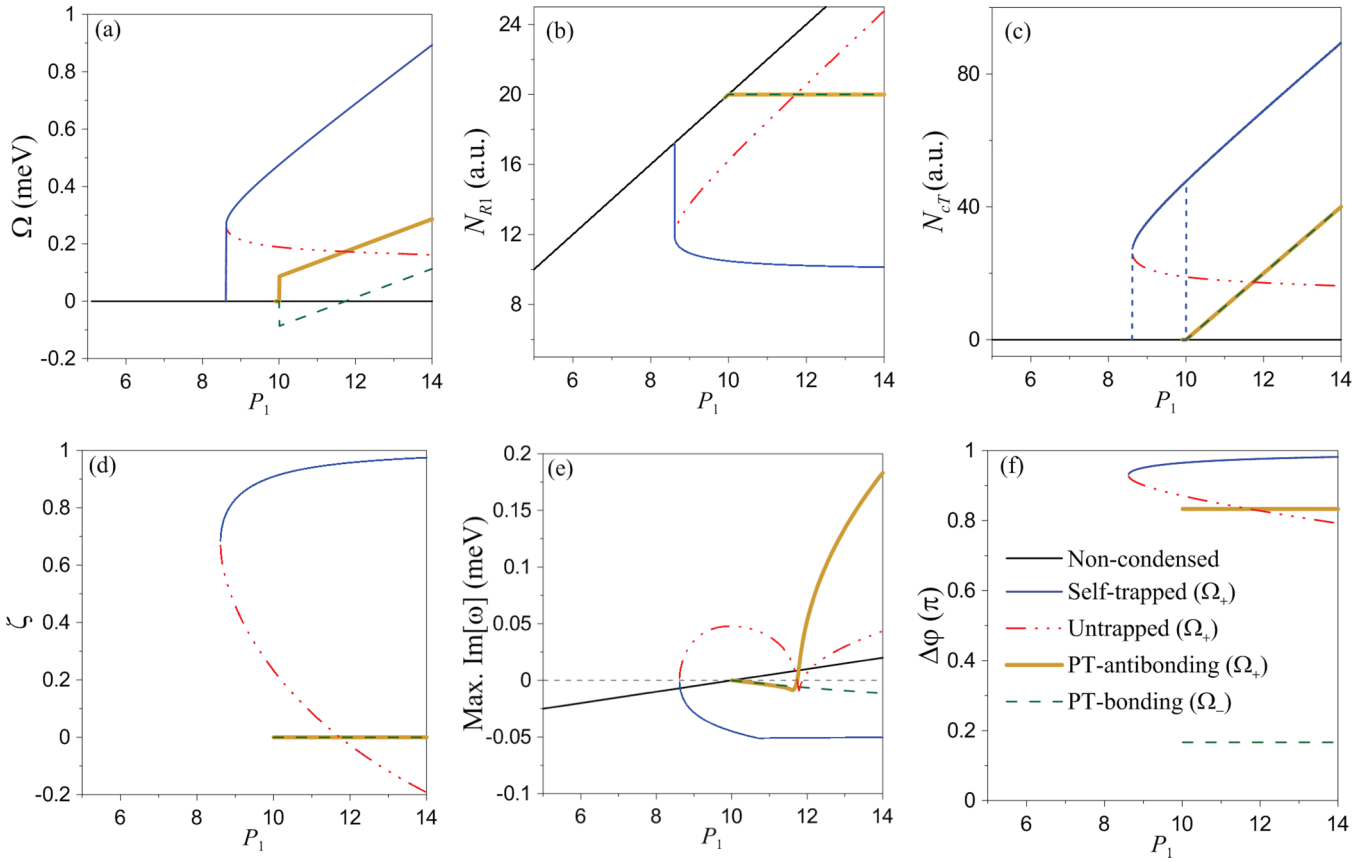

FIG. 3. (Color online) Signatures of four stationary condensate states with respect to the pumping strength P_1: (a) energy spectrum corresponding to the real eigenvalues Ω_+ or Ω_-; (b) reservoir-polariton number N_{R1} in response to the condensates; (c) total condensate-polariton number N_{cT}; (d) population imbalance ζ; (e) stability determined by the maximum imaginary part of the fluctuation spectrum; and (f) phase difference $\Delta\varphi$. These states are not necessarily orthogonal with each other due to the nonlinearity, and they can be classified into two groups. Thin solid (blue) and dash-dotted (red) curves represent the asymmetric (self-trapped and untrapped) states, and both of them are antibonding states (Ω_+) with a phase difference close to π. Thick solid (yellow) and long-dashed (green) curves correspond to the PT-symmetric states with Ω_+ and Ω_-, respectively, and they coincide in (b)–(d) except for having different energy and phase. Above the threshold, two (for large pumping) or three (for small pumping) states are stable. Below the threshold there exists a hysteresis behavior between the self-trapped state and the noncondensed state, shown by the vertical short-dashed (blue) lines in (c). The threshold pumping $P_{\rm th} = 10$ is determined by the noncondensed state, which is shown by the black lines [not shown in (d) and (f)] and becomes unstable above the threshold. Parameters used are $\epsilon_1 = \epsilon_2 = 0$, $U_1 = U_2 = 0.01$ meV, $\gamma_1 = \gamma_2 = 0.1$ meV, $\gamma_{R1} = 0.5$ meV, $R_1' = 0.01$ meV, and $J = 0.1$ meV.

analyze the dynamical stability with respect to the stationary states.

Figure 3(e) shows the maximum imaginary part of the fluctuation spectrum. One of the PT-symmetric states, Ω_-, is always stable and the other, Ω_+, becomes unstable when P_1 is increased. As for the imbalanced states, the self-trapped state is stable except for a small region below the threshold, and the other one (untrapped state) is generally unstable unless it is close to the PT state with Ω_+. This leads to multistability of the condensation resulting from polariton tunneling.

Below threshold, there exists a bistable regime with a self-trapped condensed state and a noncondensed state. The bistability can be explained by damped oscillations of the polariton BJJ. The self-trapping oscillations occur if the initial polariton number is larger than a critical value $[\tilde{U} N_{cT}(0)/2J > \Lambda_c]$, with a suitable range of the initial imbalance $\zeta(0)$ [10], and it is eventually damped to the imbalanced equilibrium position $\zeta(t \to \infty) > 0$. Otherwise, the oscillations are damped to a balanced state with $\zeta(t \to \infty) = 0$, and from the condition $\dot{N}_{cT} = 0$ in (9) the condensation must vanish unless the threshold is reached. If the pumping strength is increased from 0, the noncondensed state holds without initial condensation and becomes unstable across the threshold. The self-trapped state dominates just above the threshold due to the minute occupation of the other states. After that, the above-critical polariton number retains the condensation when the pumping decreases. Thus the hysteresis of condensation could be experimentally observed by cyclically increasing and decreasing the pumping near the threshold, provided that fluctuation of the pumping intensity is reduced, e.g., by employing a continuous-wave diode laser [28,29].

Above the threshold, the multiple stable states are also determined by the initial values. When the self-trapping condition is not satisfied, the condensates evolve to other stable states. In conserved BJJs [10], for $|\Delta\varphi(0)| \leqslant \pi/2$, the self-trapping occurs in the running-phase modes provided that $\zeta(0) > \zeta_c$,

while for $|\Delta\varphi(0)| > \pi/2$, it could be in either the running-phase modes or the π-phase modes, depending on both $N_{cT}(0)$ and $\zeta(0)$. The suitable range of $\zeta(0)$ is altered by the reservoir and the decay, and a large initial imbalance generally induces the self trapping. We have shown that, for zero detuning, the self-trapped state must be antibonding-like, with a phase difference close to π, even if the initial phase is 0 [Fig. 3(f)]. This can be understood by the fact that the running phase is damped to $(2n+1)\pi$ and eventually reaches an antibonding-like stationary state. One notes that the damped running phase and π-phase locking have been observed in a recent experiment [13]. This phenomenon seems to be different from our case because the eigenenergy is never real without pumping; i.e., no stationary condensate is achieved. In the next section we also derive an oscillator model to explain the π-phase locking either with or without the stationary condensation.

In order to experimentally observe the behavior of each stable state, an additional pulsed laser resonant with the polariton energy band is necessary to coherently excite the system, before the incoherent pumping is applied. The initial conditions of the condensate polaritons can be well controlled by exploiting this technique, where an arbitrary population imbalance in a linear combination of bonding and antibonding states can be created [13]. For comparison, another system, in which the incoherent pumping is replaced with a continuous-wave resonant laser, is discussed here. Under long-time coherent pumping, the dynamics is essentially different from our study. No reservoir polaritons are excited and the stationary states depend on the laser frequency [3]. In this case, a regime of optical bistability exists for a single condensate with a pumping frequency higher than the ground-state energy of polaritons [30]. The tunneling of a polariton BJJ, under one-side pumping, further gives rise to several unstable regimes for high pumping amplitudes. [31] However, in our study, there exists at least one stable state (zero-condensate or self-trapping state) for all pumping strengths.

IV. OSCILLATOR MODEL

A. Self-trapping regime

Figure 4 shows, for zero detuning, the π-phase locking of the self-trapped states in a nonequilibrium polariton BJJ by solving Eq. (9), either with or without stationary condensation. For the noncondensed case, our results agree well with the experiment [13]. It has been predicted that the imbalance of self-trapping eventually evolves into an oscillatory regime after the polariton number drops below the critical value [32]. However, the mechanism of π-phase locking is not understood yet.

Here, we derive a nonlinear dissipated-oscillator model from (9), with $U_{12} = 0$, in order to further understand the mechanism of this phenomenon. Under self-trapping conditions, $\eta \equiv \sqrt{1-\zeta^2(t)} \ll 1$ and $\zeta(t) \approx 1-\eta > 0$, the system can reduce to a second-order differential equation,

$$\Delta\ddot{\varphi}(t) \approx \bar{U}\dot{N}_{cT}(t) - 2J\left(\frac{1-\eta}{\eta}\right)\sin\left[\Delta\varphi(t)\right]\Delta\dot{\varphi}(t) - 2J^2\left(\frac{1}{\eta}\right)\sin[2\Delta\varphi(t)] + O(\eta), \quad (11)$$

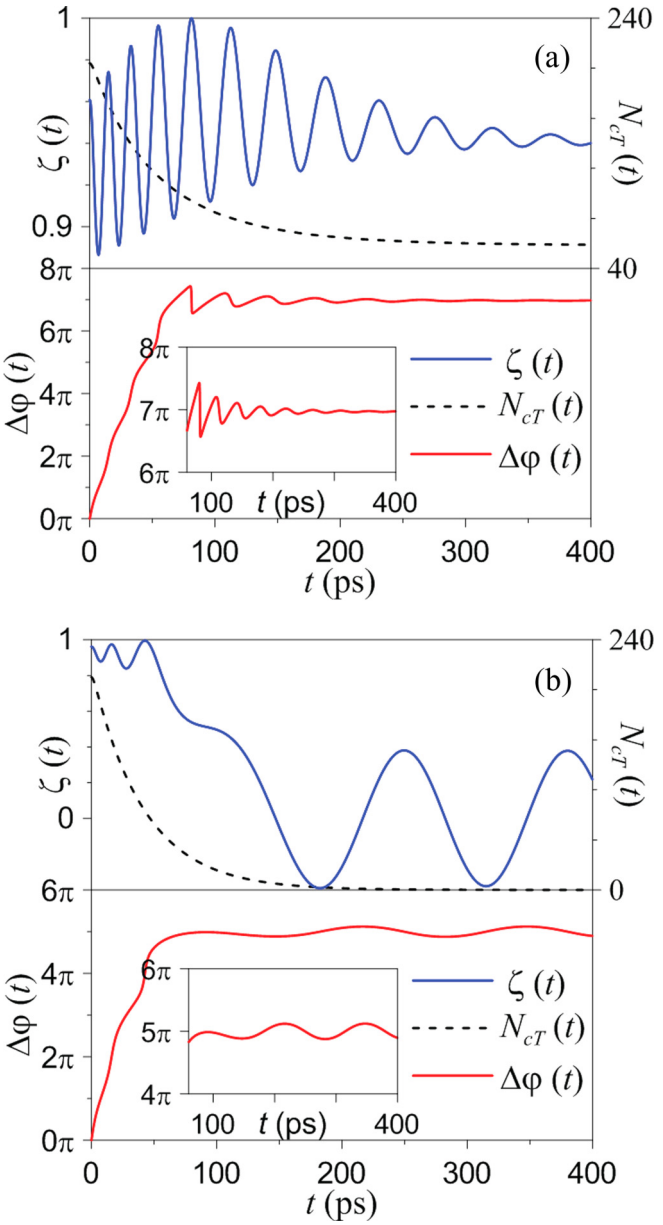

FIG. 4. (Color online) Time dependence of the imbalance $\zeta(t)$, the condensate-polariton number $N_{cT}(t)$, and the phase difference $\Delta\varphi(t)$ of the self-trapped state with zero initial phase difference for (a) $P_1 = 11$ and (b) $P_1 = 0$ (b). Insets: π-phase locking for $\Delta\varphi(t \to \infty)$.

corresponding to a pendulum with a position-dependent dissipation and a decaying driving force $\bar{U}\dot{N}_{cT}$ satisfying

$$\bar{U}\dot{N}_{cT} \approx \left[2\bar{V}^I + V_{12}^I(1-\eta)\right]\bar{U}N_{cT}. \quad (12)$$

The angle of the pendulum is defined by $2\Delta\varphi(t)$, and thus the pendulum has minimal potential energy for $\Delta\varphi = n\pi$, with n being either odd or even. The angular velocity is given by

$$\Delta\dot{\varphi} = \Delta E + 2J\left(\frac{1-\eta}{\eta}\right)\cos\left(\Delta\varphi\right), \quad (13)$$

where

$$\Delta E \equiv \epsilon_{12} + V_{12}^R + \bar{U}(1-\eta)N_{cT}. \quad (14)$$

The angular velocity can be 0 only for $\Delta\varphi \in (\pi/2, 3\pi/2)$, because $\Delta E > 0$ for zero detuning ($\epsilon_{12} + V_{12}^R = 0$). Hence the pendulum is stable for odd n. If the initial angular velocity is low, the pendulum oscillates with a low amplitude around the π phase. Otherwise, it moves with an increasing phase. The driving force is able to decelerate the running phase and to lock the π phase before $\bar{U}\dot{N}_{cT} \approx 0$, as long as $N_{cT}(0)$ is large enough.

This model can also be extended to the regime of nonzero detuning. From the condition $\Delta E > 0$ in Eq. (13), the π-phase locking holds for positive detuning and small negative detuning, i.e., $\epsilon_{12} + V_{12}^R > -\bar{U}N_{cT}$. Otherwise, the phase will be locked around 0 for large negative detuning. Thus, we can unify the phase-locking phenomenon for both the condensed and the noncondensed cases. A main difference between these two cases is the population imbalance after the phase is locked. For the noncondensed case, N_{cT} decays to 0 and the self-trapping ($\eta \ll 1$) no longer holds. However, the phase is still locked because the angular velocity has been decelerated to be small.

B. Josephson regime

In contrast to the self-trapping regime, the dynamics of ac Josephson oscillations can be investigated in the limit of $|\zeta| \ll 1$. In the Josephson regime, i.e., $\bar{U}N_{cT} \gg J$, the equations of motion, (9), can be simplified as

$$\begin{aligned} \dot{\zeta} &\approx V_{12}^I - 2J\sin(\Delta\varphi), \\ \Delta\dot{\varphi} &\approx \epsilon_{12} + V_{12}^R + \bar{U}N_{cT}\zeta, \end{aligned} \tag{15}$$

with $\dot{N}_{cT} \approx 0$ and $\dot{N}_{R1} \approx 0$. This model mimics a superconducting Josephson junction applied by an extra dc current source $V_{12}^I > 0$ due to the one-side pumping. For zero detuning $\epsilon_{12} + V_{12}^R = 0$, the population is balanced and the states possess PT symmetry, as long as the current source is smaller than the critical current $2J$. This corresponds to the dc Josephson effect, where the phase differences for bonding and antibonding states are determined by the ratio of V_{12}^I and $2J$, with $0 < \sin(\Delta\varphi) \leqslant 1$. If $V_{12}^I > 2J$, the population imbalance will deviate from the limit of $|\zeta| \ll 1$ by charging across the junction and, eventually, evolve to the self-trapped state. This is exactly the spontaneous PT-symmetry breaking from Eq. (7).

For the cases of equivalent pumping ($V_{12}^I = 0$) [17,18], the condensates are desynchronized when the detuning is larger than a critical value, resembling the ac Josephson effect driven by a bias voltage. However, the dc current source results in a finite average charging rate $\langle\dot{\zeta}(t)\rangle > 0$, which either balances the bias voltage to lock the running phase in the Josephson regime or drives the population into the self-trapping regime. Therefore, the ac oscillations in our study are washed out by the dc current drive, and the condensates are always synchronized. Although the stationary population is asymmetric in the presence of detuning, a phenomenon similar to the spontaneous PT-symmetry breaking can still take place since the charging rate $\dot{\zeta}$ is dominated by the competition between V_{12}^I and $2J$.

V. DISCUSSION

A. Detuning effects

It is important to consider the interaction between the condensate and the reservoir polaritons, as well as that between the condensate polaritons and the high-energy excitons, which, above threshold, are responsible for the blue shift of the polariton energy band of the order of milli–electron volts [33]. Under one-side pumping, the blue shift of the pumped side induces an energy difference across the polariton BJJ. On the other hand, a difference in the confinement potential between the pillars might take place during the fabrication process. These effects contribute to the effective detuning term $\Delta\varepsilon_{12} \equiv \epsilon_{12} + V_{12}^R$ in Eq. (9).

In order to analyze the detuning effects, all particle numbers of the stationary states can be represented as functions of the stimulated scattering R_1, i.e.,

$$\begin{aligned} N_{c1} &= N_{c1}(R_1) \geqslant 0, \\ N_{R1}(R_1) &= \frac{R_1}{R_1'} \geqslant 0, \\ N_{c2}(R_1) &= \frac{R_1 - \gamma_1}{\gamma_2} N_{c1}(R_1) \geqslant 0, \end{aligned} \tag{16}$$

and the corresponding pumping can be derived from Eq. (4), i.e.,

$$P_1(R_1) = \gamma_{R1}N_{R1}(R_1) + R_1 N_{c1}(R_1) \geqslant 0. \tag{17}$$

The condensate number of the first site N_{c1} and the pumping strength P_1 are solved by $\Omega_{\pm}[N_{c1}(R_1), R_1] \in \mathbb{R}$ from Eq. (6), as shown in Fig. 5. In general, the states with $R_1 \gg \gamma_1 + \gamma_2$ (0.2 meV here) are unstable since they are close to the noncondensed states.

In the presence of detuning, the PT-symmetric states and the asymmetric states are hybridized near the threshold. Figure 2(b) shows that the threshold of a polariton BJJ reduces to that of a single condensate upon increasing $|\Delta\varepsilon_{12}|$. This is similar to the mechanism that the Rabi oscillations in a double-quantum-dot system are suppressed by detuning. For positive detuning, the self-trapped state is still antibonding and appears at a lower pumping strength [dashed dark gray (blue) curve close to $R_1 = 0.1$ in Fig. 5]. The other states appear with a finite polariton number at a higher pumping strength. For negative detuning, the bonding state with zero phase dominates the self-trapping near the threshold [dash-dotted light gray (red) curve close to $R_1 = 0.1$], and it becomes more PT-symmetric (close to $R_1 = 0.2$) when the the antibonding states [dash-dotted dark gray (blue) curve] emerge with increasing P_1. These are related to the previously discussed criterion $\Delta E > 0$ of π-phase locking. The interactions between condensate polaritons and incoherent polaritons (and excitons) contribute to a positive detuning ($V_{12}^R > 0$). Due to the reduced threshold, the bistability below P_{th} could become insignificant. However, a negative potential difference $\epsilon_{12} < 0$ can recover this bistable regime.

At a high condensate density, the hybridization becomes weak, and all the states reduce asymptotically to PT-symmetric and asymmetric states without detuning. Nonlinear effects, such as the long-time self trapping and the spontaneous PT-symmetry breaking, eventually reduce to the situation in

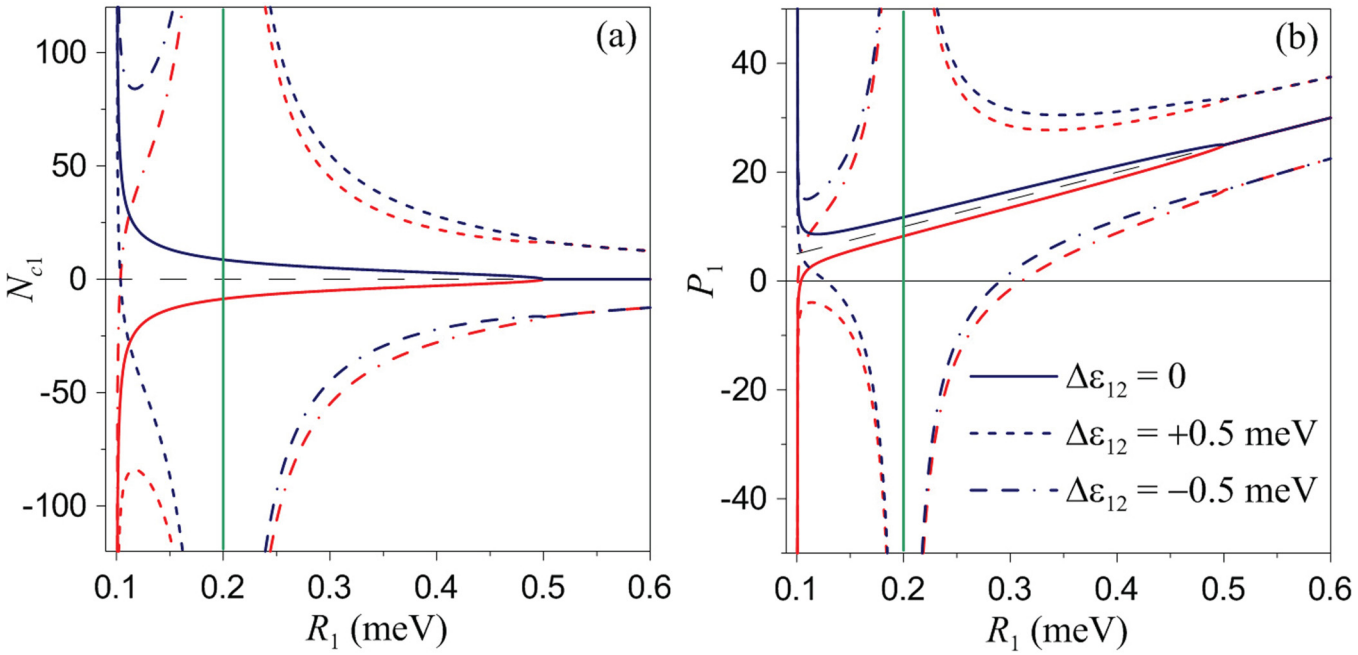

FIG. 5. (Color online) Detuning effects of the stationary states: (a) number N_{c1} of condensate polaritons at the pumped side for stationary solutions with $R_1 \geqslant \gamma_1 = 0.1$ meV and (b) corresponding pumping P_1, both as functions of the stimulated scattering R_1 for three detunings, $\Delta\varepsilon_{12} \equiv \epsilon_{12} + V_{12}^R$. Dark gray (blue) and light gray (red) curves represent antibonding (Ω_+) and bonding (Ω_-) asymmetric states, respectively. The vertical solid (green) line corresponds to both the PT-symmetric states ($\Omega_\pm$) for zero detuning. These solutions make sense only for $N_{c1} \geqslant 0$ and $P_1 \geqslant 0$, i.e., the upper half-plane in (a) and the area above the thin dashed line (corresponding to $P_1 = \gamma_{R1} N_{R1}$) in (b). The detuning introduces hybridization and anticrossing between the PT-symmetric and the asymmetric states and changes the dynamics for small pumping. However, increasing the pumping strength would restore the zero-detuning behavior, i.e., the bistability of the self-trapped state and the PT-symmetric bonding state.

III. One notes that, in the presence of detuning, the condition of PT symmetry $E_1 = E_2^*$ cannot be satisfied. However, PT-symmetry-like states can still exhibit similar signatures, as discussed in Sec. IV B. Therefore, the polariton BJJ, as a macroscopic quantum system, can be used to experimentally investigate PT-symmetry breaking by tuning the center-to-center distance between two pillars, where this phenomenon has been observed only for classical systems that mimic a non-Hermitian Hamiltonian [25].

B. Photoluminescence

Our results provide further insight into the micropillar experiment [20], where several states with different energies are found above the threshold in the spectrally resolved emission distribution. Similar phenomena were also observed in CdTe microcavities with spatial photonic potential disorder [28,29]. This phenomenon can be attributed to the coexistence of multiple stable states resulting from incoherent initial conditions or noises [28,34]. When the initial condition is not specifically controlled by an additional resonant pumping as in Ref. [13], the fluctuations of population imbalance and phase difference could cause simultaneous condensation into multiple stable states. This can be analyzed by adding a noise term to the Gross-Pitaevskii equation [34].

Figure 6 shows simulations of the spectrally resolved emission distribution from the stable states in Fig. 3. Although the interactions among these states are ignored in our simplified model, the signatures in the experiment in Ref. [20] can still be qualitatively captured by the multistability. Close to the threshold [Fig. 6(a)], there are three available states, i.e., the PT-symmetric states (both bonding and antibonding) at the two bottom levels as well as the self-trapped state at the highest level. The self-trapped state has a much stronger condensation than the other two states, owing to the localization of the stimulated scattering. A spatial shift of both the bottom states to the unpumped site was observed in the experiment, and this can be attributed to the repulsive interactions with the self-trapped states and the pumping spot.

At high pumping [Fig. 6(b)], the antibonding symmetric state becomes unstable, and the emission spectrum is dominated by the self-trapped state and the bonding symmetric state. As mentioned, a positive detuning must be introduced by the interactions with the incoherent polaritons/excitons, leading to an imbalance of the bottom state weighted to the unpumped site, in agreement with the experimental observation. The detuning does not affect the self-trapped state much. However, the bottom state could be more localized at site 2 due to the interaction with the self-trapped state. When the pumping strength is higher, the reservoir polaritons are not accumulated more due to the depletion by condensation. On the other hand, the incoherent excitons, which are inactive to the polariton condensation, can increase with pumping, and thus the detuning increases. As the number of condensate polaritons also increases, the detuning in Eq. (15) can be compensated, with a finite imbalance $\zeta < 0$. As a result, the PT-symmetric-like state exists at large pumping unless Eq. (7) is violated.

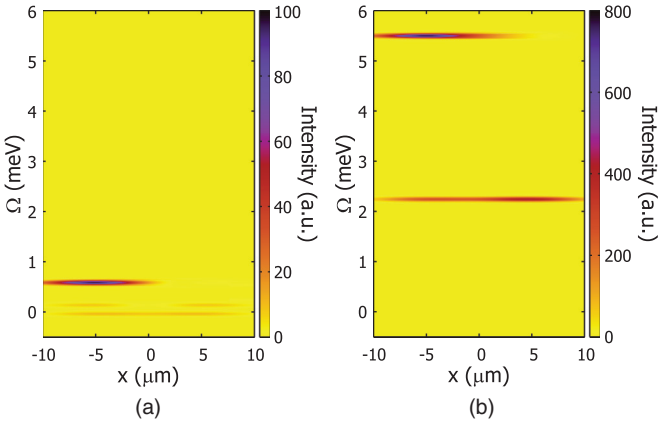

FIG. 6. (Color online) Simulation of the spectrally resolved emission distributions derived from stable states (a) close to the threshold (with $P_1 = 11$) and (b) at high pumping (with $P_1 = 50$ and an additional potential difference $\Delta\varepsilon_{12} = 1$ meV induced by the incoherent polaritons and high-energy excitons). Micropillars are centered at $x_{1/2} = \mp 5\,\mu$m, with radii of 5 μm. The emission strengths and distributions of the nth stable state $|\Psi_n(x,\Omega)|^2 = |\Psi_{1n}(x - x_1, \Omega - \Omega_n) + \Psi_{2n}(x - x_2, \Omega - \Omega_n)|^2$ are determined by its energy Ω_n, particle numbers, population imbalance, and phase difference, where the spectral and spatial distributions on each pillar $\Psi_{jn}(x - x_j, \Omega - \Omega_n)$ are defined by Gaussian functions. The three states in (a), from bottom to top, are the PT-symmetric Ω_- state, the PT-symmetric Ω_+ state, and the self-trapped state. In (b), the PT-symmetric Ω_+ state becomes unstable and only two states are left.

For microcavities with potential disorder [29], the observed emission intensity lacks the time-reversal symmetry, i.e., $I(k) \neq I(-k)$, and the phase differences of the wave functions are locked to $\pi/2$. Under equivalent pumping, with the time-reversal symmetry kept, a radiative coupling can be introduced to explain this symmetry breaking and the phase locking [34]. However, the radiative coupling seems to be unimportant for micropillars. First, the observed phase difference for self-trapping is locked to π instead of $\pi/2$ [13]. Second, introducing this coupling to our model, i.e., $J \to J + i\Gamma$, will essentially break the PT symmetry in Eq. (2) and lead to the absence of the bottom states in Fig. 6, where only the self-trapped state with a $\pi/2$ phase is left. Accordingly, Josephson coupling dominates the micropillar system and radiative coupling can be ruled out. In addition, a $\pi/2$ phase is also possible for both the PT-symmetric states near the exceptional point, where $\sin(\Delta\varphi) \approx 1$ in Eq. (15).

VI. SUMMARY

In summary, we have analyzed, within mean-field theory, the dynamics of a polariton Josephson junction pumped on one side. The reservoir polaritons contribute to the bias voltage by interaction with the condensate polaritons, as well as a dc current source by stimulated scattering together with the decay rates. In contrast to the equivalent pumping, there is no long-lived ac Josephson oscillation. Instead, the Josephson current induces multiple stable states corresponding to different initial conditions. These states can be attributed to either the self-trapping effect resulting from the nonlinearity or the PT symmetry of the system. The coexisting states with different energies and the π-phase locking observed in recent experiments can be explained by our results. We also predict the condensation and a hysteresis phenomenon below the threshold. Moreover, the spontaneous PT-symmetry breaking can be related to the competition between the dc current drive and the critical current of the junction. As a result, this macroscopic quantum system can be used to investigate this phenomenon, which has been observed only in classical systems.

ACKNOWLEDGMENTS

This work was partially supported by the National Center for Theoretical Sciences and National Science Council, Taiwan, Grant Nos. NSC 101-2628-M-006-003-MY3 and MOST 103-2112-M-006-017-MY4. F.N. was partially supported by the RIKEN iTHES Project, the MURI Center for Dynamic Magneto-Optics, and a Grant-in-Aid for Scientific Research (S).

[1] J. Kasprzak, M. Richard, S. Kundermann, A. Baas, P. Jeambrun, J. M. J. Keeling, F. M. Marchetti, M. H. Szymanska, R. Andre, J. L. Staehli, V. Savona, P. B. Littlewood, B. Deveaud, and L. S. Dang, Bose-Einstein condensation of exciton polaritons, Nature **443**, 409 (2006).

[2] R. Balili, V. Hartwell, D. Snoke, L. Pfeiffer, and K. West, Bose-Einstein condensation of microcavity polaritons in a trap, Science **316**, 1007 (2007).

[3] I. Carusotto and C. Ciuti, Quantum fluids of light, Rev. Mod. Phys. **85**, 299 (2013).

[4] M. Yamaguchi, K. Kamide, R. Nii, T. Ogawa, and Y. Yamamoto, Second thresholds in bec-bcs-laser crossover of exciton-polariton systems, Phys. Rev. Lett. **111**, 026404 (2013).

[5] C. Schneider, A. Rahimi-Iman, N. Y. Kim, J. Fischer, I. G. Savenko, M. Amthor, M. Lermer, A. Wolf, L. Worschech, V. D. Kulakovskii, I. A. Shelykh, M. Kamp, S. Reitzenstein, A. Forchel, Y. Yamamoto, and S. Hofling, An electrically pumped polariton laser, Nature **497**, 348 (2013).

[6] A. Amo, D. Sanvitto, F. P. Laussy, D. Ballarini, E. d. Valle, M. D. Martin, A. Lemaitre, J. Bloch, D. N. Krizhanovskii, M. S. Skolnick, C. Tejedor, and L. Vina, Collective fluid dynamics of a polariton condensate in a semiconductor microcavity, Nature **457**, 291 (2009).

[7] G. Tosi, G. Christmann, N. G. Berloff, P. Tsotsis, T. Gao, Z. Hatzopoulos, P. G. Savvidis, and J. J. Baumberg, Sculpting oscillators with light within a nonlinear quantum fluid, Nat. Phys. **8**, 190 (2012).

[8] G. Roumpos, M. D. Fraser, A. Loffler, S. Hofling, A. Forchel, and Y. Yamamoto, Single vortex-antivortex pair in an exciton-polariton condensate, Nat. Phys. **7**, 129 (2011).

[9] K. G. Lagoudakis, M. Wouters, M. Richard, A. Baas, I. Carusotto, R. Andre, L. S. Dang, and B. Deveaud-Pledran, Quantized vortices in an exciton-polariton condensate, Nat. Phys. **4**, 706 (2008).

[10] S. Raghavan, A. Smerzi, S. Fantoni, and S. R. Shenoy, Coherent oscillations between two weakly coupled Bose-Einstein condensates: Josephson effects, π oscillations, and macroscopic quantum self-trapping, Phys. Rev. A **59**, 620 (1999).

[11] M. Albiez, R. Gati, J. Fölling, S. Hunsmann, M. Cristiani, and M. K. Oberthaler, Direct observation of tunneling and nonlinear self-trapping in a single bosonic josephson junction, Phys. Rev. Lett. **95**, 010402 (2005).

[12] K. G. Lagoudakis, B. Pietka, M. Wouters, R. André, and B. Deveaud-Plédran, Coherent oscillations in an exciton-polariton josephson junction, Phys. Rev. Lett. **105**, 120403 (2010).

[13] M. Abbarchi, A. Amo, V. G. Sala, D. D. Solnyshkov, H. Flayac, L. Ferrier, I. Sagnes, E. Galopin, A. Lemaitre, G. Malpuech, and J. Bloch, Macroscopic quantum self-trapping and josephson oscillations of exciton polaritons, Nat. Phys. **9**, 275 (2013).

[14] D. Porras, C. Ciuti, J. J. Baumberg, and C. Tejedor, Polariton dynamics and bose-einstein condensation in semiconductor microcavities, Phys. Rev. B **66**, 085304 (2002).

[15] M. H. Szymańska, J. Keeling, and P. B. Littlewood, Nonequilibrium quantum condensation in an incoherently pumped dissipative system, Phys. Rev. Lett. **96**, 230602 (2006).

[16] M. Wouters and I. Carusotto, Excitations in a nonequilibrium bose-einstein condensate of exciton polaritons, Phys. Rev. Lett. **99**, 140402 (2007).

[17] M. Wouters, Synchronized and desynchronized phases of coupled nonequilibrium exciton-polariton condensates, Phys. Rev. B **77**, 121302 (2008).

[18] M. O. Borgh, J. Keeling, and N. G. Berloff, Spatial pattern formation and polarization dynamics of a nonequilibrium spinor polariton condensate, Phys. Rev. B **81**, 235302 (2010).

[19] A. Baas, K. G. Lagoudakis, M. Richard, R. André, L. S. Dang, and B. Deveaud-Plédran, Synchronized and desynchronized phases of exciton-polariton condensates in the presence of disorder, Phys. Rev. Lett. **100**, 170401 (2008).

[20] M. Galbiati, L. Ferrier, D. D. Solnyshkov, D. Tanese, E. Wertz, A. Amo, M. Abbarchi, P. Senellart, I. Sagnes, A. Lemaître, E. Galopin, G. Malpuech, and J. Bloch, Polariton condensation in photonic molecules, Phys. Rev. Lett. **108**, 126403 (2012).

[21] M. Wouters, I. Carusotto, and C. Ciuti, Spatial and spectral shape of inhomogeneous nonequilibrium exciton-polariton condensates, Phys. Rev. B **77**, 115340 (2008).

[22] E.-M. Graefe, Stationary states of a PT symmetric two-mode Bose–Einstein condensate, J. Phys. A **45**, 444015 (2012).

[23] H. Cartarius and G. Wunner, Model of a $\mathcal{PT}$-symmetric Bose–Einstein condensate in a δ-function double-well potential, Phys. Rev. A **86**, 013612 (2012).

[24] C. M. Bender, Making sense of non-hermitian hamiltonians, Rep. Prog. Phys. **70**, 947 (2007).

[25] B. Peng, S. K. Özdemir, F. Lei, F. Monifi, M. Gianfreda, G. L. Long, S. Fan, F. Nori, C. M. Bender, and L. Yang, Parity-time-symmetric whispering-gallery microcavities, Nat. Phys. **10**, 394 (2014).

[26] B. Peng, K. Özdemir, S. Rotter, H. Yilmaz, M. Liertzer, F. Monifi, C. M. Bender, F. Nori, and L. Yang, Loss-induced suppression and revival of lasing, Science **346**, 328 (2014).

[27] H. Jing, S. K. Özdemir, X.-Y. Lü, J. Zhang, L. Yang, and F. Nori, $\mathcal{PT}$-symmetric phonon laser, Phys. Rev. Lett. **113**, 053604 (2014).

[28] A. P. D. Love, D. N. Krizhanovskii, D. M. Whittaker, R. Bouchekioua, D. Sanvitto, S. A. Rizeiqi, R. Bradley, M. S. Skolnick, P. R. Eastham, R. André, and L. S. Dang, Intrinsic decoherence mechanisms in the microcavity polariton condensate, Phys. Rev. Lett. **101**, 067404 (2008).

[29] D. N. Krizhanovskii, K. G. Lagoudakis, M. Wouters, B. Pietka, R. A. Bradley, K. Guda, D. M. Whittaker, M. S. Skolnick, B. Deveaud-Plédran, M. Richard, R. André, and L. S. Dang, Coexisting nonequilibrium condensates with long-range spatial coherence in semiconductor microcavities, Phys. Rev. B **80**, 045317 (2009).

[30] A. Baas, J. P. Karr, H. Eleuch, and E. Giacobino, Optical bistability in semiconductor microcavities, Phys. Rev. A **69**, 023809 (2004).

[31] D. Sarchi, I. Carusotto, M. Wouters, and V. Savona, Coherent dynamics and parametric instabilities of microcavity polaritons in double-well systems, Phys. Rev. B **77**, 125324 (2008).

[32] I. A. Shelykh, D. D. Solnyshkov, G. Pavlovic, and G. Malpuech, Josephson effects in condensates of excitons and exciton polaritons, Phys. Rev. B **78**, 041302 (2008).

[33] A. S. Brichkin, S. I. Novikov, A. V. Larionov, V. D. Kulakovskii, M. M. Glazov, C. Schneider, S. Höfling, M. Kamp, and A. Forchel, Effect of coulomb interaction on exciton-polariton condensates in gaas pillar microcavities, Phys. Rev. B **84**, 195301 (2011).

[34] I. L. Aleiner, B. L. Altshuler, and Y. G. Rubo, Radiative coupling and weak lasing of exciton-polariton condensates, Phys. Rev. B **85**, 121301 (2012).